Cancer Immunology, Immunotherapy (2025) 74:177
https://doi.org/10.1007/s00262-025-04028-w

RESEARCH

Identification and validation of poor prognosis immunoevasive subtype of esophageal cancer with tumor-infiltrating SAMD3 + NK cell abundance

Xu Huang[1,2,5] · Runze You[1,2,5] · Fangyi Liu[3,5] · Zitao Jian[1,2,5] · Guanyou Zhou[3,5] · Hao Yin[1,2,5] · Mengyuan Wu[1,2,5] · Tiantao Sun[1,2,5] · Zhiyun Duan[1,2,5] · Wenyi Xu[1,2,5] · Shaoyuan Zhang[1,2,5] · Xinyu Yang[1,2,5] · Heng Jiao[1,2,5] · Shuyi Yang[2,4,5] · Qingle Wang[2,4,5] · Jun Yin[1,2,5] · Han Tang[1,2,5] · Miao Lin[1,2,3,5] · Lijie Tan[1,2,3,5]

Received: 30 October 2024 / Accepted: 19 March 2025

Abstract

Introduction Esophageal cancer (EC) remains highly lethal due to tumor microenvironment (TME)-mediated immune evasion. While natural killer (NK) cells are central to antitumor immunity, their functional states in EC are poorly characterized.

Methods We integrated bulk RNA-seq (TCGA/GEO) and single-cell data to construct an NK cell-derived prognostic signature (NK score) via LASSO-Cox regression. Immunofluorescence was applied to assess the clinical relevance of SAMD3 + NK cells in EC. Using both xenograft mouse models and in vitro co-culture procedures, the impact of SAMD3 on NK cell function was confirmed.

Results In EC patients, the prognostic NK score—which is generated from important NK cell markers including SAMD3—was substantially correlated with a worse chance of survival. NK cells within the TME had significant levels of SAMD3 expression, as seen by immunofluorescence labeling. Moreover, NK cells with SAMD3 knockdown exhibited enhanced antitumor activity, leading to decreased tumor development in the xenograft model.

Discussion Our results demonstrate the predictive significance of NK cell markers in EC and pinpoint SAMD3 as a critical modulator of NK cell activity. We pioneer SAMD3 + NK cells as architects of TME immunosuppression in EC. Our findings nominate SAMD3 inhibition as a combinatorial strategy to overcome immune checkpoint blockade resistance.

Keywords Esophageal cancer · Natural killer cell · SAMD3

Xu Huang, Runze You, Fangyi Liu, Zitao Jian have been contributed equally to this work.

✉ Miao Lin
linmiao@fudan.edu.cn

✉ Lijie Tan
tan.lijie@zs-hospital.sh.cn

1 Departments of Thoracic Surgery, Zhongshan Hospital, Fudan University, Shanghai, China

2 Cancer Center, Zhongshan Hospital, Fudan University, Shanghai, China

3 The School of Basic Medical Sciences, Fudan University, Shanghai, China

4 Departments of Radiology, Zhongshan Hospital, Fudan University, Shanghai, China

5 Departments of Thoracic, Zhongshan Hospital (Xiamen), Fudan University, Xiamen, China

Abbreviations

ACT	Adjuvant chemotherapy
DEGs	Differentially expressed genes
EC	Esophageal cancer
HR	Hazard ratio
ICIs	Immune checkpoint inhibitors
LASSO	Least absolute shrinkage and selection operator
OS	Overall survival
PD-1	Programmed cell death protein 1
TCGA	The cancer genome atlas
TFE	Three-field esophagectomy
TME	Tumor microenvironment
WCGNA	Weighted gene co-expression network
ZSHS	Zhongshan Hospital

Published online: 19 April 2025

Introduction

Esophageal cancer (EC) is the sixth most prevalent cause of cancer-related death worldwide and the eighth most common type of cancer overall [1]. Esophageal squamous cell carcinoma (ESCC) and esophageal adenocarcinoma (EAC) are the two main types of this cancer that manifest [2]. East Asia and Africa are the regions with higher incidence of ESCC, the more common subtype, while wealthy countries are more likely to experience EAC [3, 4]. The prognosis for EC is still dismal despite major breakthroughs in care, such as endoscopic resection, chemoradiotherapy, and new immunotherapies [5–7]. This is mostly because of the tumor's aggressiveness and heterogeneity, as well as our incomplete knowledge of its molecular underpinnings. These difficulties highlight the critical need for research aimed at determining the molecular etiology of EC and discovering new biomarkers, as these efforts may result in more effective treatments and better patient outcomes. Furthermore, investigating the immune system's involvement in cancer may offer additional understanding into innovative therapeutic approaches [8].

A new and exciting era in anticancer treatment has been brought about by the immune checkpoint inhibitor (ICI)-based immunotherapy's rapid development in recent years [9–11]. Due to the distinct tumor microenvironment (TME) of esophageal cancer and the intricate individual heterogeneity of the disease, only a small percentage of patients with esophageal cancer receive long-lasting benefits from ICI medicines, despite these advancements [12]. Therefore, improving clinical outcomes for esophageal cancer patients and designing more individualized ICI treatment plans depend heavily on thoroughly characterizing the TME features and building reliable predictive models [13, 14].

An essential part of the innate immune system, natural killer (NK) cells are crucial for the body's defense against malignancies [15]. NK cells do not require prior sensitization to recognize and kill malignant cells. Certain indicators that play a critical role in controlling NK cell activation and immunological state are required for the detection and measurement of NK cells within the tumor microenvironment [16]. Comprehending the function of these markers is essential in clarifying the processes that govern NK cell-mediated cytotoxicity, providing valuable perspectives on possible remedial approaches to strengthen immune responses against cancer.

The molecule known as SAMD3, or sterile alpha motif domain-containing protein 3, has gained attention because of its distinct expression pattern and possible connections to immune cell function [17]. Unlike the well-studied SMAD3, SAMD3 remains poorly understood [18]. Numerous physiological functions, including translational regulation, cell cycle control, and protein interactions, are impacted by the SAMD protein family [19]. SAMD3 may be essential for the maturation and differentiation of NK cells, as evidenced by the high expression of the protein in memory CD8 T cells and NK cells, which are essential for immunological responses [20]. The therapeutic relevance of SAMD3 and its possible impact on NK cell modulation in EC, however, were yet unknown.

In this study, the function of NK cells in esophageal cancer (EC) was methodically examined. From EC datasets, we extracted important NK cell markers to create a predictive signature (NK score), which was verified in other datasets. This signature demonstrated the significance of NK cell markers in EC prognosis by showing that patients with higher risk scores had significantly worse survival rates. This is also the first study that raises the possibility that SAMD3 + NK cells could be a sign of a bad prognosis. The decreased antitumor cytotoxicity of SAMD3 + NK cells may have contributed to the immune-suppressive tumor microenvironment, setting the stage for further investigation into SAMD3 targeting in EC.

Method

Study cohorts

The Cancer Genome Atlas (TCGA) cohort enrolled 173 patients from TCGA. RNA-seq data for esophageal cancer were obtained from the UCSC database with corresponding clinical information. Additionally, gene expression data for esophageal cancer were downloaded from the GEO database, specifically datasets GSE53624 and GSE53622, comprising 119 and 60 patients, respectively, along with their clinical information [21].

Following approval by the Clinical Research Ethics Committee of Zhongshan Hospital (ZSHS), the ZSHS cohort comprised 180 patients with ESCC treated with "three-field esophagectomy" (TFE). Patients were included into this study under the following criteria: (a) informed consent; (b) available of clinicopathological data; (c) pathologically diagnosed as ESCC; and (d) without preoperative systemic treatment. The Helsinki Declaration II was followed for the design of the study and the testing techniques. All tumor tissue samples were formalin-fixed and paraffin-embedded (FFPE). Clinicopathological characteristics were retrospectively collected including age, sex, tumor location, tumor size, tumor grade, and application of platinum-based ACT.

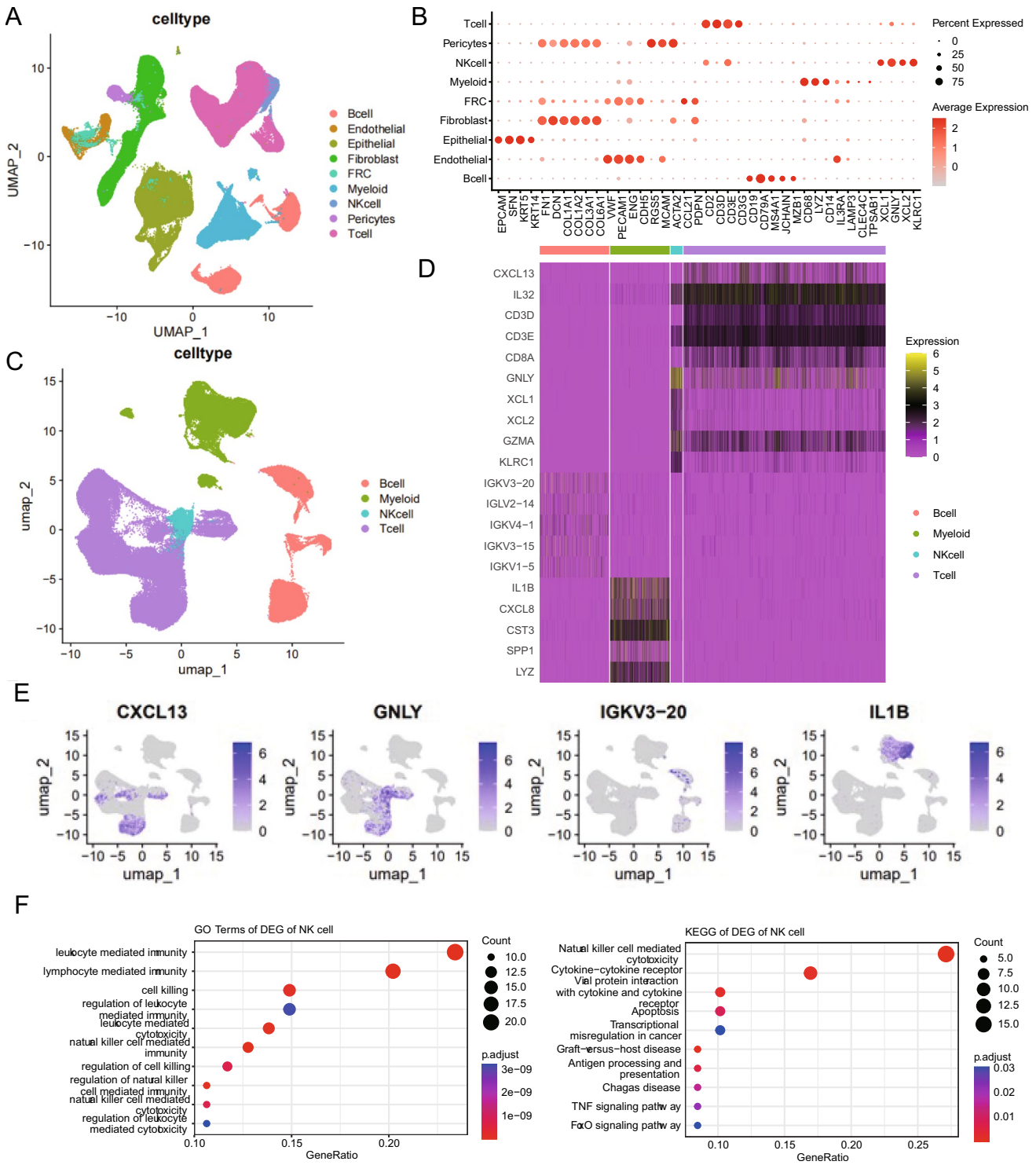

Fig. 1 Immune landscape and phenotypic characteristics of tumor-infiltrating NK cells in esophageal cancer patients. **A** UMAP plot showing all cell types. **B** Expression levels of marker genes across different cell types. **C** UMAP plot displaying all immune cell types. **D** Heatmap illustrating the expression levels of immune cell marker genes. **E** UMAP plot indicating the distribution of immune cell marker gene expression. **F** Functional enrichment analysis of NK cell-specific genes

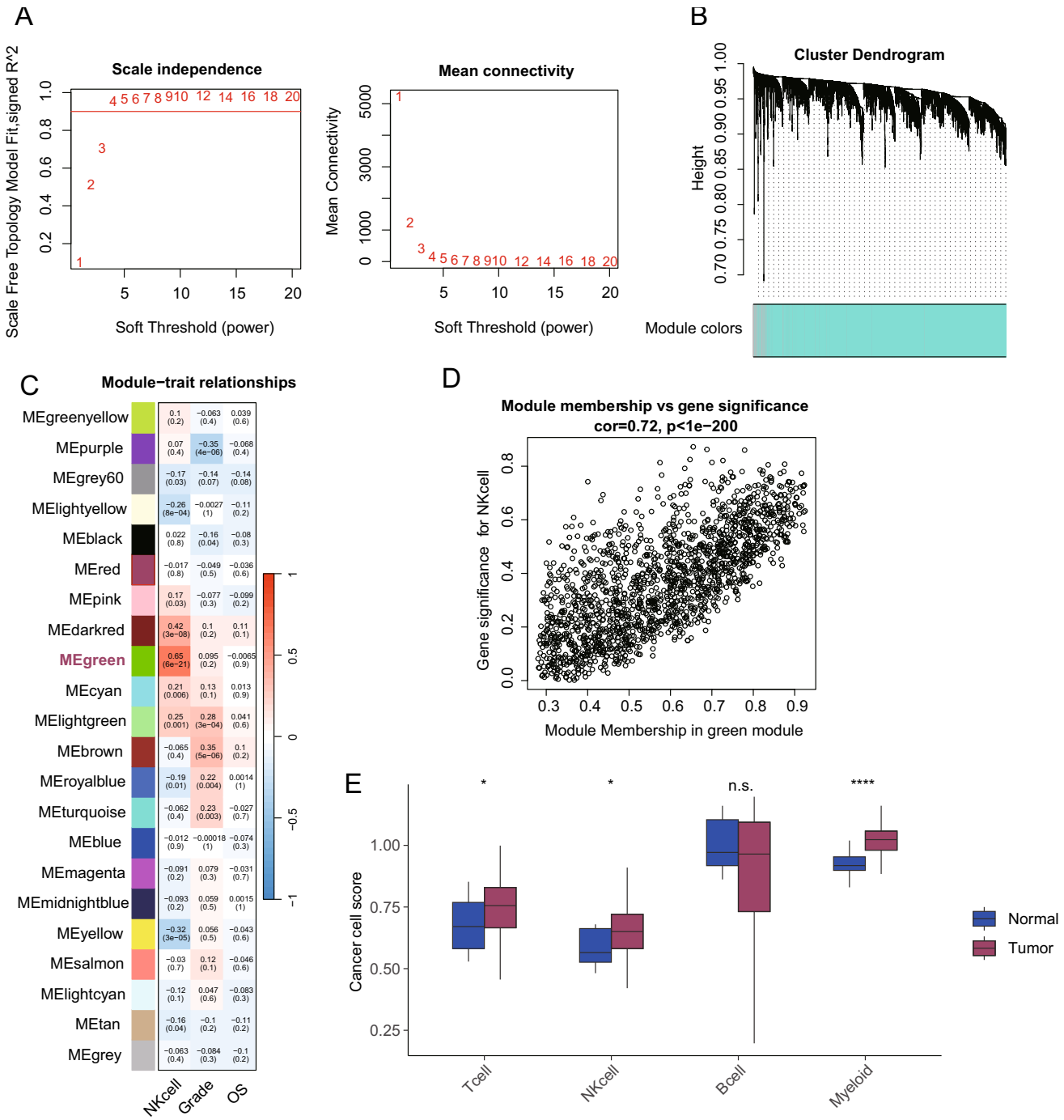

Fig. 2 Extraction of esophageal cancer tumor-infiltrating NK cell-specific genes. **A** Determination of the appropriate soft threshold: network topology analysis. **B** Module visualization. **C** WGCNA heatmap showing the correlation between modules and traits. **D** Scatter plot displaying the correlation between traits and gene expression levels. **E** Proportional differences of NK cells between tumor and normal samples. The *P* values were calculated by the Mann–Whitney U test. $*P<0.05$, $**P<0.01$, $***P<0.001$

Single-cell RNA-seq data process and analysis

The scRNA-seq data of 60 primary esophageal cancer (EC) samples were downloaded from the GSE160269 dataset [22]. For analysis, Seurat (version 4.1.1) was employed. Initial processing involved the creation of Seurat objects for CD45-negative and CD45-positive cell populations. Cells with more than 4000 detected genes were filtered out to remove potential doublets, and cells with fewer than 500 detected genes or with mitochondrial

genome content greater than 10% were excluded. The Harmony algorithm was applied to adjust for potential batch effects [23]. Subsequent clustering of cells was done using the "FindClusters" function with a resolution of 0.5, followed by visualization in two-dimensional space using t-distributed stochastic neighbor embedding (t-SNE) and Uniform Manifold Approximation and Projection (UMAP). Cell populations were manually annotated based on feature markers. Differentially expressed genes (DEGs) for each cell type were identified using the "FindAllMarkers" function with default parameters. Functional enrichment analysis for DEGs in NK cells, T cells, B cells, and myeloid cells was performed using clusterProfiler, with GO and KEGG pathway analyses conducted using enrichGO and enrichKEGG functions, respectively.

Bioinformatics analysis

Weighted gene co-expression network analysis (WGCNA) was used to identify gene modules and candidate biomarkers from TCGA data, with thresholds set at MM > 0.6 and GS > 0.2. The CIBERSORT algorithm and ssGSEA were employed to analyze the tumor microenvironment [24, 25]. Differentially expressed genes were subjected to GO and KEGG enrichment analysis using the clusterProfiler package ($P < 0.05$). CellChat was used to infer cell–cell communication networks, utilizing the default CellChatDB ligand–receptor database [26].

Construction of a prognostic NK score signature

In this study, we developed a prognostic scoring system, designated the NK score. Initially, we performed univariate Cox regression analysis on the expressions of DEGs and survival data to identify prognosis-related genes. Subsequently, we applied the least absolute shrinkage and selection operator (LASSO) and multivariate Cox regression analyses to construct an optimal predictive model [27]. The NK score was calculated using the selected genes as follows: NK score = h0(t) * exp (expression of SAMD3 * corresponding coefficient + expression of CD7 * corresponding coefficient). Patients were divided into two groups based on their NK score, with the threshold set at the median score.

Immunofluorescence assay

The detailed protocol of tumor immunofluorescence staining was carefully described in our previous studies [28]. Immunofluorescence (IF) contains antibodies against: SAMD3 (ab122028; Abcam; 1:50), CD56 (ab220360; Abcam; 1:1000). Nuclei were stained with DAPI (Sigma-Aldrich) after all the primary antigens had been labeled.

To evaluate the density of SAMD3 + cells and SAMD3 + NK cells, all the tumor microarray samples were evaluated as the average number of positive cells/HPF (at × 200 magnification) from three randomized fields by two independent pathologists who were blinded to clinicopathological data. Variations exceeding five cells in enumeration were re-evaluated by both pathologists separately to reach a final consensus.

Cell culture and reagents

Human ESCC cell lines TE-1 were obtained from Type Culture Collection Cell Bank, Chinese Academy of Sciences. The KYSE-30 cell lines were procured from the Japanese Collection of Research Bioresources (JCRB) Cell Bank. The NK-92MI cell line was kindly provided by Dr. Zhang Puran. KYSE-30 and TE-1 cells were grown in RPMI 1640 medium supplemented with 10% FBS (fetal bovine serum) and 1% penicillin/streptomycin, while NK92MI cells were maintained in α-MEM medium supplemented with 12.5% FBS, 12.5% horse serum, 0.2 mM inositol, 0.1 mM 2-mercaptoethanol, 0.02 mM folic acid, and 1% penicillin/streptomycin. The cells were cultured at 37 °C with 5% CO2. All cells have been authenticated and were tested for mycoplasma contamination.

Cell transfection

The pLKO.1-puro lentiviral plasmid was employed to prepare SAMD3 interference lentivirus. After 72 h of infection, 3 μg/ml puromycin was used for screening cells with SAMD3 knockdown. Fluorescence microscope was used to detect GFP and to analyze the efficiency of lentivirus-mediated transgenesis. Western blotting was employed to assess the efficacy of the lentivirus-mediated SAMD3 silencing in NK cells.

Western blotting

Cells were harvested by scraping into an SDS sample buffer containing a cocktail of protease inhibitors and PhosSTOP Phosphatase Inhibitor (Roche, Pleasanton, CA, USA). Western blotting was conducted in accordance with the standard procedure. The abundance of SAMD3 (ab122028; Abcam) and GAPDH (60,004–1-Ig; Proteintech) was investigated.

In vitro intervention assay

For the co-culture experiments, SAMD3 knockdown was achieved in NK92MI cells using lentiviral shRNA, followed by selection with puromycin to establish stable knockdown

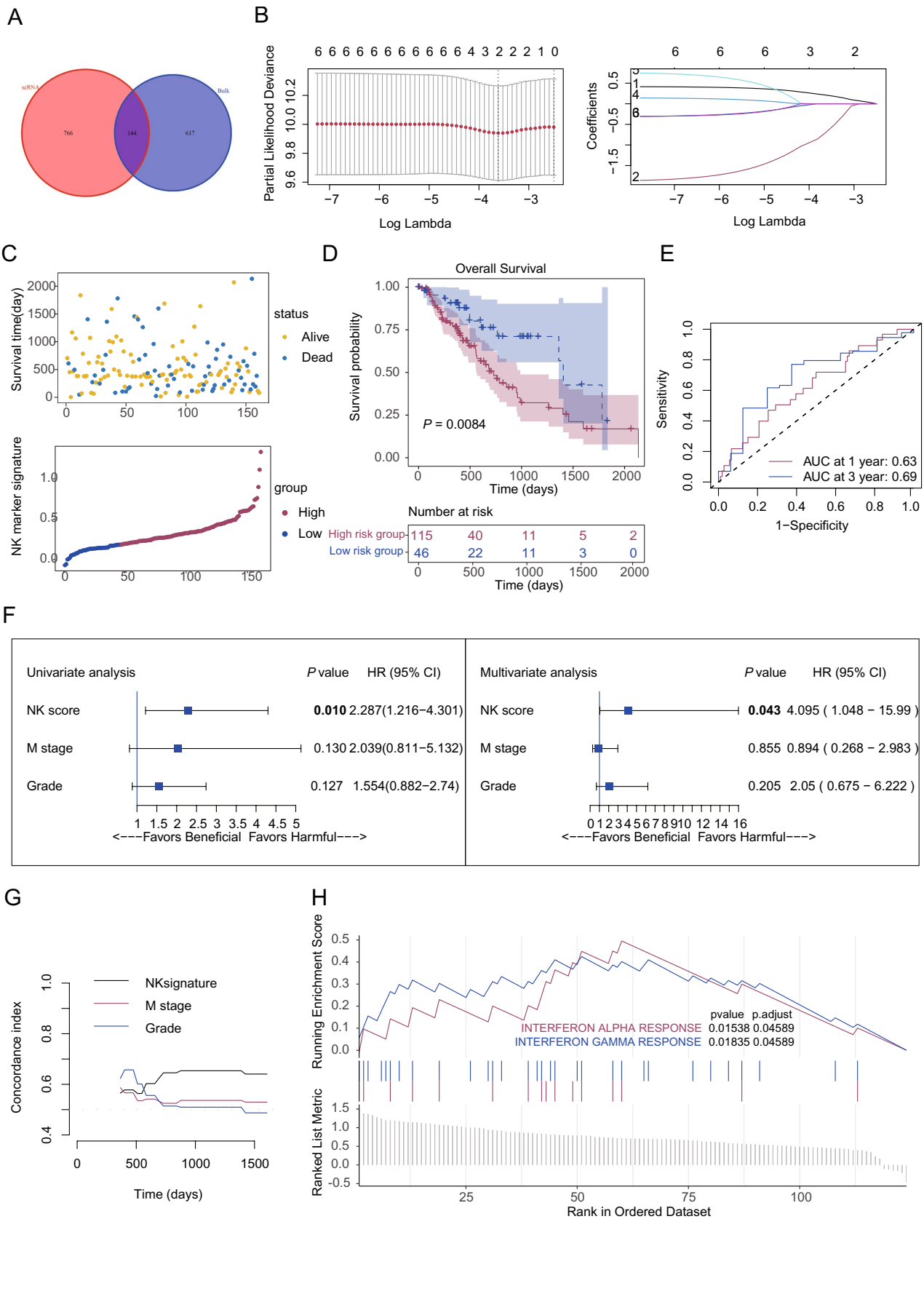
A
scRNA
Bulk
766
144
617
B
Partial Likelihood Deviance
Log Lambda
Coefficients
Log Lambda
C
Survival time(day)
status
Alive
Dead
NK marker signature
group
High
Low
D
Overall Survival
Survival probability
P = 0.0084
Time (days)
Number at risk
High risk group 115 40 11 5 2
Low risk group 46 22 11 3 0
Time (days)
E
Sensitivity
1−Specificity
AUC at 1 year: 0.63
AUC at 3 year: 0.69
F
Univariate analysis P value HR (95% CI)
NK score 0.010 2.287(1.216−4.301)
M stage 0.130 2.039(0.811−5.132)
Grade 0.127 1.554(0.882−2.74)
<---Favors Beneficial Favors Harmful--->
Multivariate analysis P value HR (95% CI)
NK score 0.043 4.095 (1.048 − 15.99)
M stage 0.855 0.894 (0.268 − 2.983)
Grade 0.205 2.05 (0.675 − 6.222)
<---Favors Beneficial Favors Harmful--->
G
Concordance index
NKsignature
M stage
Grade
Time (days)
H
Running Enrichment Score
pvalue p.adjust
INTERFERON ALPHA RESPONSE 0.01538 0.04589
INTERFERON GAMMA RESPONSE 0.01835 0.04589
Ranked List Metric
Rank in Ordered Dataset

◂**Fig. 3** Development of a NK-related predictive signature. **A** Venn diagram showing the overlap between differentially expressed genes (DEGs). **B** Left: Plot showing the coefficient changes for each feature as lambda varies. Right: Confidence interval of the selected parameter after cross-validation. **C** Scatter plot showing the distribution of NK score and survival status. **D** Kaplan–Meier analysis of overall survival (OS) for patients in high and low NK score groups. **E** Receiver operating characteristic (ROC) curves evaluating the predictive performance of NK score for 1-year and 3-year survival. **F** Univariate and multivariate Cox regression analysis based on NK score. **G** Comparison of the C-index between prognostic NK score and other clinical predictive indicators. **H** GSEA analysis of interferon function associated with NK score. Log-rank test was conducted for Kaplan–Meier curves

cell lines. Tumor cells (KYSE-30 or TE-1) were seeded into 6-well plates at a density of 1 × 10^5 cells per well and allowed to adhere overnight. The following day, NK92MI cells (either SAMD3 knockdown or control) were added to the wells at an effector-to-target (E-T) ratio of 2:1. The co-cultures were incubated for 24 h at 37 °C in a 5% CO2 atmosphere. After incubation, apoptosis in the tumor cells was assessed using an Annexin V-FITC/PI apoptosis detection kit according to the manufacturer's instructions. Flow cytometry was used to analyze the percentage of apoptotic cells.

In vivo intervention assay

To investigate the interaction between tumor cells and immune cells in vivo, we performed co-culture experiments using a xenograft mouse model. Human esophageal cancer cell lines KYSE-30 were cultured under standard conditions. NK92MI cells, an NK cell line, were maintained and transduced with shRNA targeting SAMD3 using a lentiviral vector to establish stable knockdown cell lines. Male NOD/SCID mice aged 6–8 weeks were subcutaneously injected with 1 × 10^6 KYSE-30 cells suspended in Matrigel to establish xenograft tumors. When tumors reached approximately 100 mm^3, mice were randomly assigned to receive intravenous injections of either SAMD3 knockdown NK92MI cells or control NK92MI cells (1 × 10^6 cells per injection) twice a week. Tumor growth was monitored by measuring tumor size with calipers, and tumor volume was calculated. At the end of the treatment period, mice were euthanized, and tumors were harvested for further analysis.

Statistical analysis

Statistical analysis was performed using IBM SPSS (version 21.0), R software (version 4.3.1), and GraphPad Prism (version 8.0). The median value of the SAMD3 + NK cells density was adopted as the cutoff point. Continuous variables were analyzed with Student's t test or Mann–Whitney U test. Pearson's χ^2 test was applied to compare categorical variables. Kaplan–Meier curves, Log-rank test, and Cox proportional hazards regression analysis were used to determine clinical significance. Data were shown as mean ± SD. A two-tailed $P < 0.05$ was considered as statistically significant.

Results

Immune landscape and phenotypic characteristics of tumor-infiltrating NK cells in EC (Esophageal Cancer) patients

To explore the tumor microenvironment landscape in esophageal cancer, we obtained a single-cell dataset of 60 patients with esophageal cancer (GSE160269) from the GEO database. After quality control, we acquired 208,659 high-quality cells. Based on known cell markers, we identified nine cell types (Fig. 1A, B). Subsequently, we visualized 65,378 T cells, 22,477 B cells, 3900 NK cells, and 19,273 myeloid cells using UMAP (Fig. 1C). Heatmap and UMAP show the distribution of specific marker genes in tumor-infiltrating immune cells (Fig. 1D, E). Subsequently, we performed enrichment analysis for immune cell-specific gene functions (Figs. 1F and S1). Notably, for NK cells, in addition to cytotoxic pathways, we observed enrichment in immune regulation and cytokine signaling pathways, suggesting potential functional alterations in NK cells within EC.

Extraction of esophageal cancer tumor-infiltrating NK cell-specific genes

We obtained the RNA-seq dataset for esophageal cancer from the TCGA database, including 162 tumor samples and 11 normal samples. Using ssGSEA and immune cell-specific genes, we assessed the infiltration levels of immune cells in each sample. Next, we constructed a weighted gene co-expression network (WGCNA) based on the gene transcription profiles of all tumor samples to identify modules significantly associated with NK cell traits and key NK cell markers (Fig. 2A, B). We identified 22 modules, with the green module showing the strongest correlation with NK cells, indicating that the green module is significantly associated with NK cell traits (Fig. 2C). Finally, we characterized the correlation between genes in the green module and NK cell infiltration abundance (Fig. 2D). We also observed that both NK and T cells were higher in tumors, suggesting their potential role in shaping the tumor-associated microenvironment (TAM) (Fig. 2E).

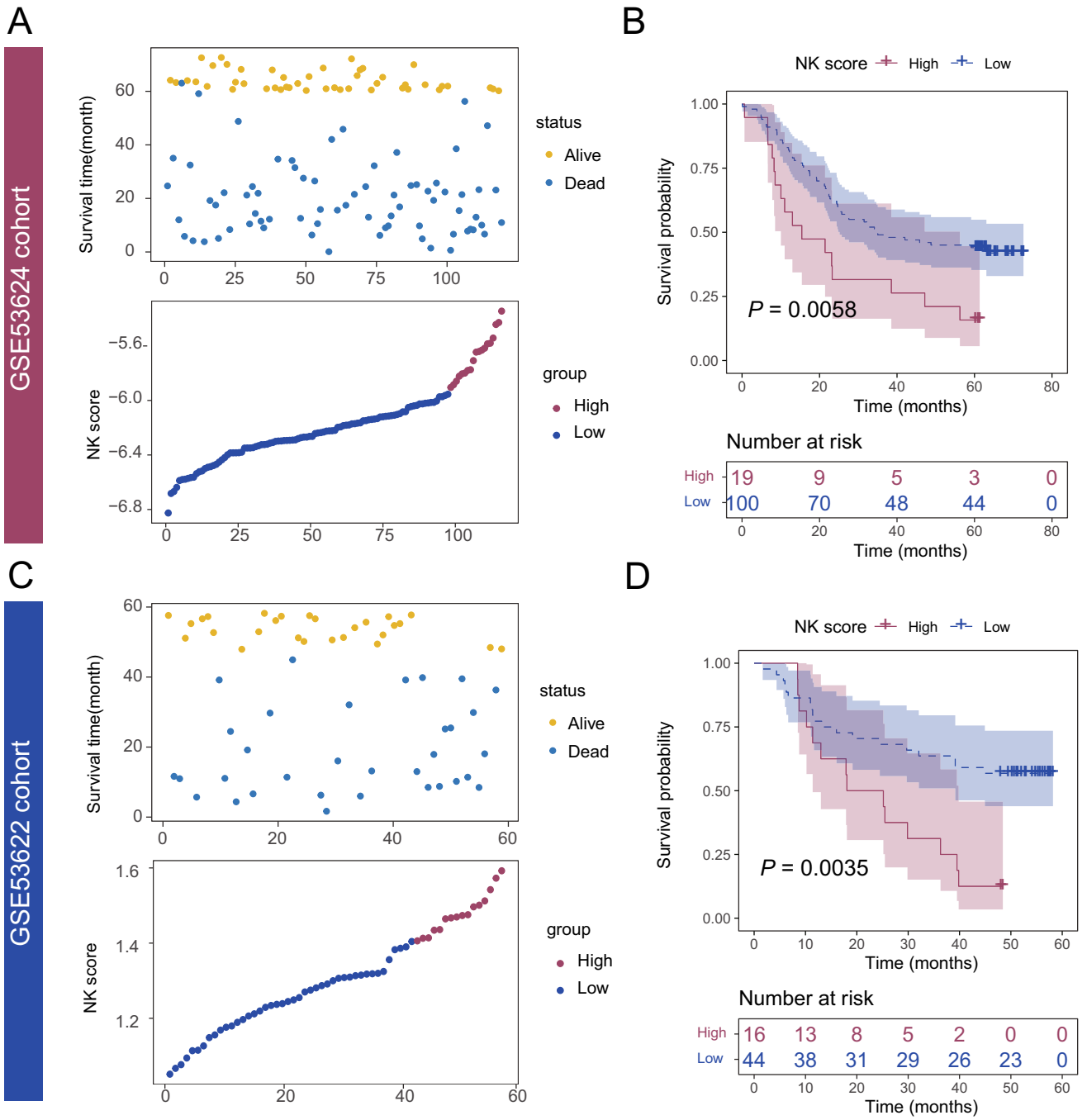

Fig. 4 External validation of the predictive ability of the NK score. **A** Scatter plot showing the distribution of NK score and survival status in GSE53624 cohort. **B** Kaplan–Meier analysis of OS for patients in GSE53624 cohort. **C** Scatter plot showing the distribution of NK score and survival status in GSE53622 cohort. **D** Kaplan–Meier analysis of OS for patients in GSE53622 cohort

Development and validation of a NK-related predictive signature

From the single-cell dataset, we identified 910 differentially expressed genes in NK cells. Using bulk RNA sequencing data, we identified 761 key NK cell markers. Intersecting these datasets yielded 144 NK cell-related markers (Fig. 3A). To identify prognostically relevant NK cell markers, we conducted univariate Cox regression analysis, resulting in the identification of six markers: CD7, SAMD3, BIN2, MS4A7, GRAP2, and SIRPG.

Subsequently, we employed LASSO regression to refine the prognostic model, isolating CD7 and SAMD3 as the critical NK cell markers (Fig. 3B). To validate the reliability, we performed functional enrichment analysis on these two key NK cell markers and found enrichment in functions such as phagocytosis and phosphor-tyrosine residue binding (Figure S2A). Consistent clustering of esophageal cancer samples based on these markers identified two NK-related subtypes (Figure S2B). The M1 subtype, characterized by high expression of CD7 and SAMD3, was associated with significantly poorer survival outcomes (Figure S2C, D). Based on the LASSO results, we developed a prognostic risk score model using these key NK markers, stratifying patients into high-risk and low-risk groups. Notably, patients in the high-risk group exhibited significantly poorer prognoses (Fig. 3C, D).

We further assessed the prognostic efficacy of the NK score, demonstrating its robust predictive capability for 1-year and 3-year survival in esophageal cancer patients (Fig. 3E). Univariate and multivariate Cox regression analyses confirmed the NK score as an independent prognostic factor significantly associated with survival outcomes (Fig. 3F). Comparative analysis of the C-index revealed that the NK score outperformed other clinical predictive indicators (Fig. 3G). Finally, Gene Set Enrichment Analysis (GSEA) indicated that genes highly expressed in the high-risk NK score group were significantly enriched in the interferon alpha response and interferon gamma response pathways (Fig. 3H).

In consideration of clinicopathological characteristics, it is found that the high-risk NK score group had a significantly higher proportion of patients with M1 stage disease. Additionally, clinicopathological features such as T4 stage, Stage IV, and G3 grade were more prevalent in the high-risk NK score group (Figure S3A). Furthermore, patients with M1 stage disease exhibited significantly higher NK scores (Figure S3B).

For assessing the predictive performance of the NK score, we obtained RNA-seq data for esophageal cancer from the GEO database, specifically datasets GSE53624 and GSE53622 to serve as external independent validation cohorts. In these independent validation cohorts, we observed that patients in the high-risk NK signature group exhibited significantly poorer prognoses, corroborating the predictive efficacy of the NK score (Fig. 4).

SAMD3 + NK cells indicate poor prognosis and chemotherapeutic response in EC

Alterations in the immune microenvironment are pivotal in influencing patient prognosis. To elucidate the intrinsic immune remodeling mechanisms contributing to the prognostic disparities between patients with high and low NK scores, we analyzed the differential immune cell infiltration between these groups. Our analysis revealed that the high NK score group exhibited significantly elevated levels of CD8 + T cells (Figure S4A). Furthermore, this group showed higher expression of immune checkpoint molecules, including CD274, CD40LG, CTLA4, IDO1, IDO2, LAG3, and LAIR1 (Figure S4B), indicating a substantial presence of dysfunctional effector immune cells. Additionally, cell–cell interaction analysis identified strong interactions in the TGF-β signaling pathway between NK cells and CD8 + T cells in esophageal cancer (Figure S5), which has been previously associated with immune evasion. Given that SAMD3, expressed on NK cells, is a key prognostic marker that may play a critical role in NK cell maturation and differentiation, we hypothesize that SAMD3 + NK cells represent a subset of NK cells with diminished cytotoxicity. This reduction in cytotoxic function likely contributes to immune evasion in these patients.

Next, we tried to assess the identity of SAMD3 + cells in EC. SAMD3 was found to be essentially expressed on NK cells and CD8 T cells across all cell types in scRNA-seq data (Figs. 1C and 5A). Furthermore, we performed immunofluorescence staining on samples from the ZSHS cohort. As shown in Fig. 5B, SAMD3 is prominently expressed on NK cells. The proportion of SAMD3 + NK cells was higher in stage III patients compared to stage I-II patients, while their distribution did not differ significantly across different tumor grades (Fig. 5C-E). Kaplan–Meier curves and log-rank tests indicated that high levels of SAMD3 + NK cells were associated with poorer prognosis (Fig. 5F). Considering the pivotal role of platinum-based chemotherapy in esophageal cancer treatment, we assessed the biomarker significance of SAMD3 + NK cells in patients receiving adjuvant chemotherapy (ACT) (Fig. 5G). Our findings suggest that SAMD3 + NK cells are predictive of treatment response. Conclusively, these results indicate that SAMD3 + NK cells are associated with poor prognosis and chemotherapeutic response in esophageal cancer.

While the immunofluorescence findings in the ZSHS cohort revealed stage-dependent SAMD3 + NK cell accumulation (Fig. 5C-E) and significant survival stratification ($P = 0.012$, Fig. 5F), the sample size limits subgroup analyses by histological grade. Nevertheless, the concordance between protein-level quantification (IF) and transcriptional profiles from larger cohorts (TCGA, n = 160; GSE53625, n = 179) strengthens the biological validity of these associations. Future multicenter studies with extended sample sizes are needed to refine cutoff values for clinical translation.

SAMD3 + NK cells demonstrate reduced antitumor cytotoxicity in EC

We first extracted T cells from the scRNA-seq data and re-clustered them to get Tregs and distinct clusters of CD8 + T

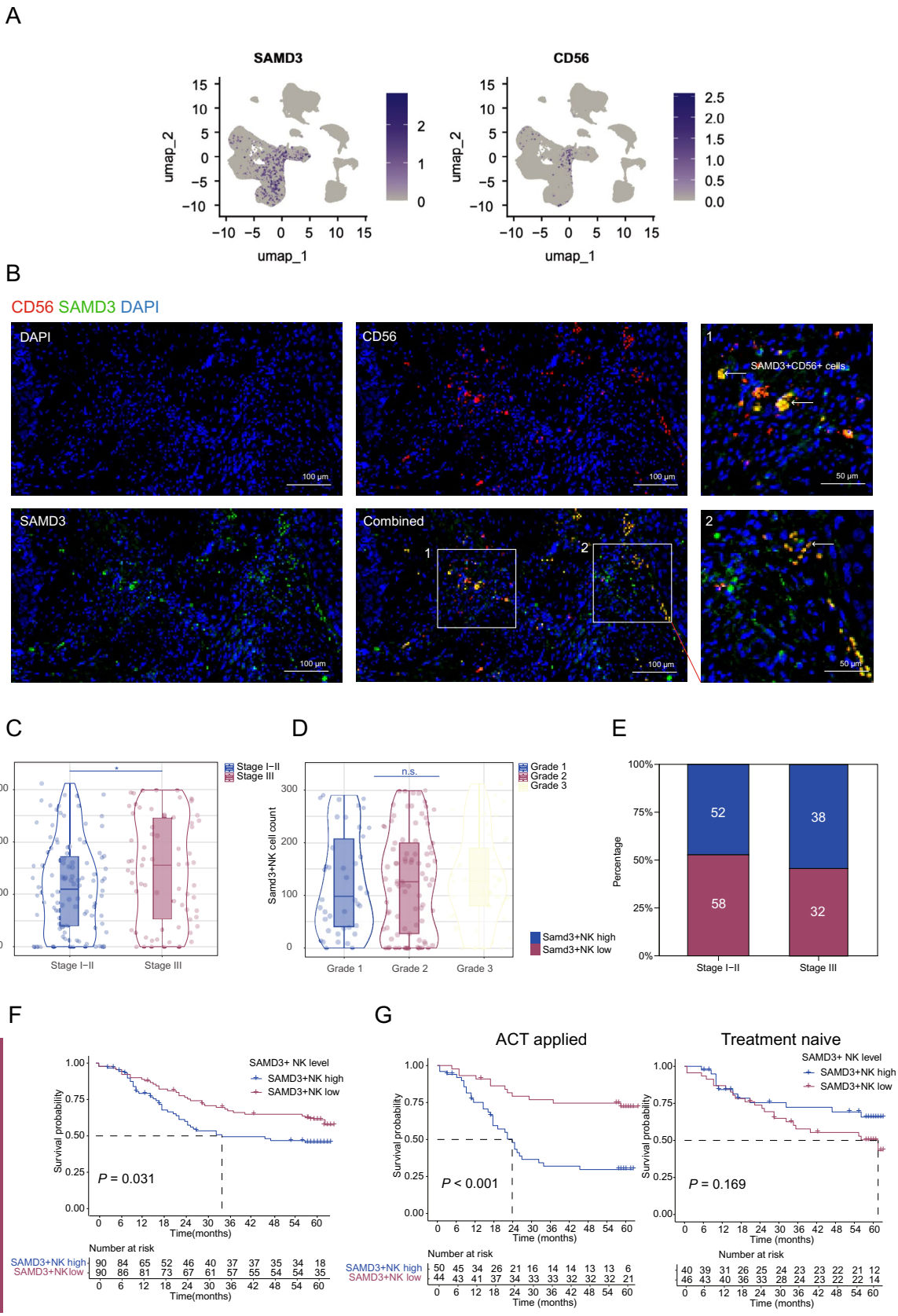
A
SAMD3
CD56
umap_1
umap_2
B
CD56 SAMD3 DAPI
DAPI
CD56
SAMD3+CD56+ cells
SAMD3
Combined
100 μm
50 μm
C
Samd3+NK cell count
Stage I–II
Stage III
D
n.s.
Grade 1
Grade 2
Grade 3
Samd3+NK high
Samd3+NK low
E
Percentage
52
58
38
32
F
ZSHS cohort
SAMD3+ NK level
SAMD3+NK high
SAMD3+NK low
Survival probability
P = 0.031
Number at risk
Time(months)
G
ACT applied
Treatment naive
P < 0.001
P = 0.169
Time (months)

◂**Fig. 5** SAMD3$^+$ NK cells yield poor prognosis and attenuated chemotherapeutic response in EC. **A** UMAP plot showing SAMD3 and CD56 mRNA expression across all cell types from 60 primary EC tumor tissues. **B** Representative immunofluorescence staining of SAMD3 (green), CD56 (red), and DAPI (blue) in FFPE EC tissues (scale bar, 100 μm). SAMD3$^+$ NK cells are circled with white frame (scale bar of the magnified image, 50 μm). **C**–**E** Statistical analysis of SAMD3$^+$ NK cells in patients with different stages and grades. **F** Kaplan–Meier curves showing the OS based on SAMD3$^+$ NK cells infiltration level in ZSHS cohort ($N=180$). **G** Kaplan–Meier curves demonstrated responsiveness to platinum-based ACT in patients from ZSHS cohort. The P values were calculated by the Mann–Whitney U test. $^*P<0.05$, $^{**}P<0.01$, $^{***}P<0.001$. Log-rank test was conducted for Kaplan–Meier curves

cells. The cell–cell interaction analysis was conducted, and strong interactions between SAMD3 + NK cells and exhausted CD8 T cells were observed, which indicated that SAMD3 + NK cells might contribute to CD8 + T cell dysfunction (Fig. 6A).

To investigate the phenotype of SAMD3 + NK cells in esophageal cancer (EC), we knocked down SAMD3 in the NK92MI cell line and co-cultured these cells with esophageal cancer cell lines KYSE-30 and TE-1 (Fig. 6B). Assessment of apoptosis in the esophageal cancer cells revealed that SAMD3 knockdown significantly enhanced the antitumor activity of NK92MI cells (Fig. 6C). Subsequently, we established a CDX model of esophageal cancer and introduced NK92MI cell interventions in vivo (Fig. 6D). Our results demonstrated that tumors in the group receiving shSAMD3 NK92MI interventions exhibited slower growth and were smaller in size (Fig. 6E-H). In summary, both in vitro and in vivo experiments confirmed that SAMD3 diminishes NK cell cytotoxicity, thereby reducing their antitumor capabilities and promoting immune evasion.

Discussion

For decades, there has been no fundamental breakthrough in the treatment of esophageal cancer worldwide. Surgery and adjuvant therapies remain the mainstay of treatment, and esophageal cancer continues to be a tumor with poor prognosis and challenging to treat. Fortunately, immunotherapies targeting the PD-1/PD-L1 axis have shown potential efficacy in various tumors, including esophageal cancer [29]. Ongoing clinical trials of first-line or adjuvant/neoadjuvant treatments, such as KEYNOTE-975, PALACE-2 (NCT04435197), and CheckMate-577, have been highly encouraging [30–32]. However, not all patients benefit from adjuvant therapies due to the complex interplay and dysfunctions of different cell types in the TME, which are not yet fully understood. Therefore, there is a pressing need for new models and targeted therapies. These would guide more personalized treatment strategies and facilitate improvements in the clinical efficacy of comprehensive therapy for EC.

With the rapid development of single-cell RNA sequencing technologies, researchers are increasingly exploring the molecular characteristics of tumor-infiltrating immune cells in the TME. However, most current studies have focused on adaptive immune cells, while the roles of innate immune cells have not yet received sufficient attention [33]. This oversight may significantly affect prognosis and treatment response, particularly with immunotherapy [34]. The abundance of tumor-infiltrating NK cells is closely associated with the prognosis of patients with various solid tumors [35]. In this study, we aimed to explore the NK cell marker genes in esophageal cancer (EC) through scRNA-seq analysis. By integrating multi-cohort transcriptomic data (scRNA-seq: $N=60$; bulk RNA-seq: TCGA $N=173$, GEO $N=179$), we identified 144 NK cell-related marker genes and established the NK score—a robust prognostic signature validated across platforms. While these sample sizes including immunofluorescence validation in the ZSHS cohort remain relatively small, the consistency of SAMD3 + NK cell associations with immune dysfunction reinforces their clinical relevance. Using univariate Cox regression and LASSO regression, we developed a novel prognostic prediction signature based on NK cell marker genes (NK score) for EC patients in the TCGA database, which was well validated in two independent cohorts from the GEO dataset. The NK score primarily involves two key prognostic genes for esophageal cancer, SAMD3 and CD7. A higher NK score is often indicative of poorer prognosis, and ROC curve analysis demonstrated that this score could effectively predict 1-year and 3-year survival outcomes. Additionally, multivariate Cox regression and C-index analyses indicated that the NK score is a superior prognostic marker, independent of M stage and tumor grade.

Encouraged by the excellent predictive performance of the prognostic model, we sought to explore the mechanisms behind its reshaping of the immune microenvironment. We observed that patients in the high NK score group exhibited increased infiltration of CD8 + T cells and NK cells, along with higher levels of immune checkpoints, suggesting an environment enriched with dysfunctional immune effector cells. In the current study, we discovered that SAMD3 was preferentially expressed on NK cells in EC. The abundance of SAMD3 + NK cells was correlated with poor prognosis and attenuated chemotherapeutic response in patients with locally advanced disease. Our data suggested that SAMD3 + NK cells possessed a reduced cytotoxic phenotype, as evidenced by co-culture experiments with EC tumor cells in vitro. Additionally, in vivo experiments demonstrated that inhibiting SAMD3 in NK cells enhanced their antitumor activity, providing a novel approach for targeting NK cells in cancer therapy.

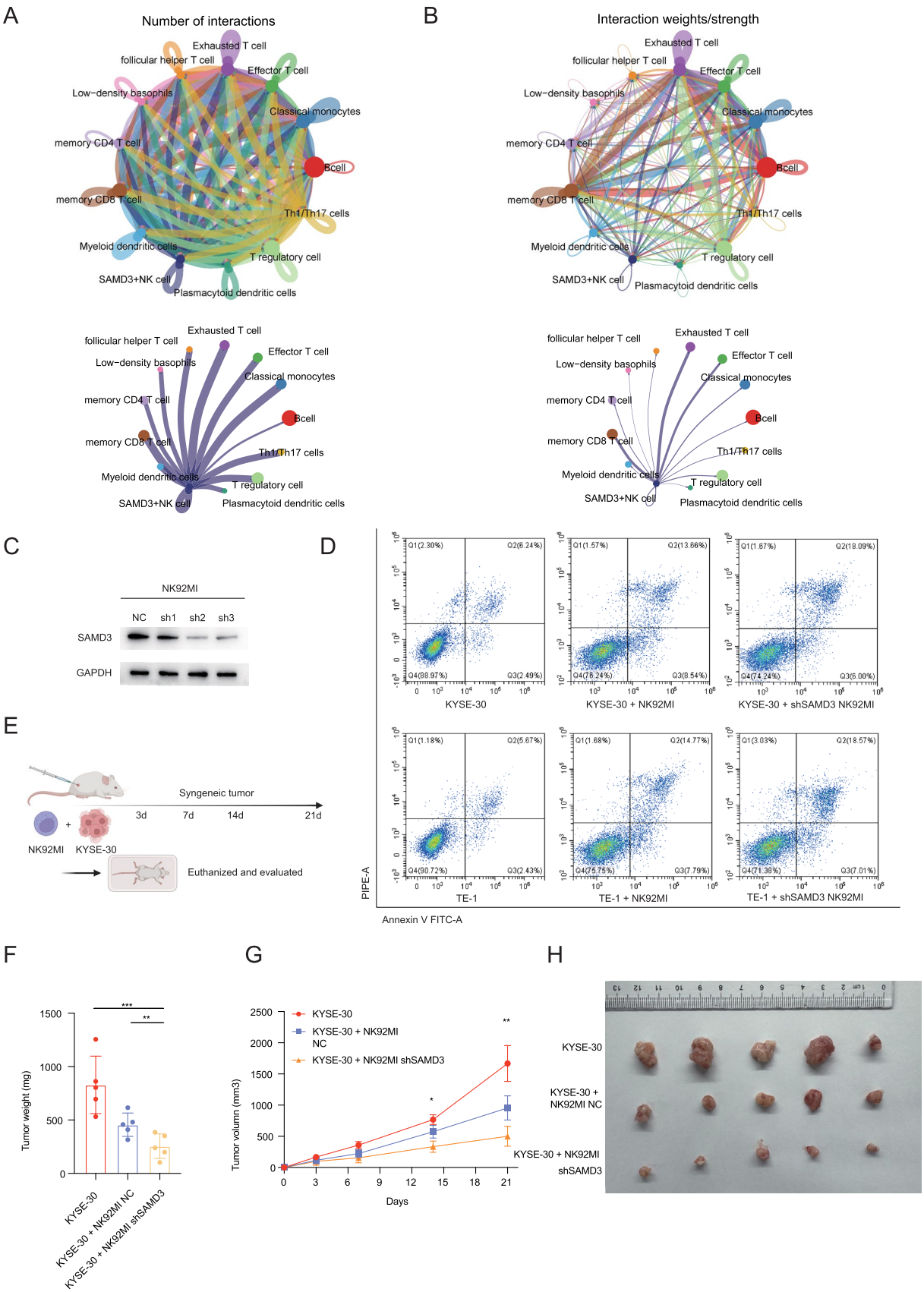
A
Number of interactions
Exhausted T cell
follicular helper T cell
Effector T cell
Low−density basophils
Classical monocytes
memory CD4 T cell
Bcell
memory CD8 T cell
Th1/Th17 cells
Myeloid dendritic cells
T regulatory cell
SAMD3+NK cell
Plasmacytoid dendritic cells
B
Interaction weights/strength
C
NK92MI
NC
sh1
sh2
sh3
SAMD3
GAPDH
D
KYSE-30
KYSE-30 + NK92MI
KYSE-30 + shSAMD3 NK92MI
TE-1
TE-1 + NK92MI
TE-1 + shSAMD3 NK92MI
PIPE-A
Annexin V FITC-A
E
Syngeneic tumor
3d
7d
14d
21d
NK92MI
KYSE-30
Euthanized and evaluated
F
Tumor weight (mg)
KYSE-30
KYSE-30 + NK92MI NC
KYSE-30 + NK92MI shSAMD3
G
Tumor volumn (mm3)
Days
KYSE-30
KYSE-30 + NK92MI NC
KYSE-30 + NK92MI shSAMD3
H
KYSE-30
KYSE-30 + NK92MI NC
KYSE-30 + NK92MI shSAMD3

◂**Fig. 6** SAMD3 + NK cells demonstrate reduced antitumor cytotoxicity in EC. **A**–**B** Chord plot demonstrating the interactions between SAMD3 + NK cells and immune cell clusters. **C** Western blot analysis of SAMD3 protein expression levels in NK92MI cells. **D** Flow cytometry analysis of apoptosis in KYSE-30 and TE-1 cells after co-culture with NK cells. **E** Flowchart outlining the in vivo validation of SAMD3$^+$ NK cells. **(F–H)** Tumor growth and size in xenograft models with NK92MI cell SAMD3 knockdown and control groups. *P* values were calculated using the Mann–Whitney U test. $^*P < 0.05$, $^{**}P < 0.01$, $^{***}P < 0.001$

Moreover, leveraging high-dimensional scRNA-seq data, we uncovered the underlying molecular mechanisms explaining the specific cell–cell interactions of SAMD3 + NK cells with dysfunctional CD8 + T cells.

While our study delineates the immunosuppressive role of SAMD3 + NK cells in esophageal cancer (EC), emerging evidence reveals conserved mechanisms of NK cell dysfunction across solid tumors. In breast cancer, NK cells recognize stress ligands via NKG2D, with cytokine priming enhancing cytolytic activity [36]. In colorectal cancer (CRC), antibody-dependent cellular cytotoxicity (ADCC) mechanisms, such as cetuximab-induced EGFR blockade, engage FcγRIII (CD16) on NK cells to trigger tumor lysis [37]. In non-small cell lung cancer (NSCLC), dual blockade of inhibitory receptors restores NK cell-mediated tumor control, paralleling our findings in EC where SAMD3 inhibition may rewire the NK cell activation–inhibition equilibrium [38].

There are two major difficulties in applying NK cell-associated immunotherapy in solid tumors: addressing NK cells to the tumor and enhancing NK cell cytotoxicity and viability [39]. Therefore, the strategy of targeting SAMD3 can be combined with immune agonists, other immune checkpoints, or drugs related to enhancement of NK cell recruitment/residency. Research has demonstrated that mesothelin-specific (CAR)-NK cells, which are known to secrete IL-2Rβγ agonist, Neo-2/15, can effectively counteract immunosuppressive polarization. This may, in turn, result in a more prolonged anti-tumoral immune response when employed in conjunction with SAMD3 inhibitors [40]. Furthermore, combining SAMD3 blockade with GSDMD agonists may mimic the "hot tumor" conversion strategies seen in immunotherapy-resistant models [41]. These parallels underscore the translational potential of our findings beyond EC, while emphasizing the need for context-specific biomarker validation.

While our findings provide valuable insights into the role of NK cells and SAMD3 in EC, it is important to acknowledge several limitations. The primary issue is the lack of appropriate mouse-derived cell lines for EC to build an immune-competent mouse model, necessitating further research to investigate the specific immune functions of SAMD3 + NK cells. Secondly, while LASSO-Cox modeling with cross-validation reduced overfitting risks, the NK score requires prospective validation in uniformly treated cohorts. The Cox model's assumptions, though statistically verified, may oversimplify risk dynamics in molecularly distinct EC subtypes. Third, differences in treatment and background among the various cohorts may introduce bias. Finally, as the conclusions are derived from retrospective studies, prospective studies are needed to yield more robust evidence. We advocate for future studies to verify the potential of targeting SAMD3 to improve antitumor efficacy, particularly when combined with PD-1 inhibitors, within the framework of more extensive clinical research.

Supplementary Information The online version contains supplementary material available at https://doi.org/10.1007/s00262-025-04028-w.

Acknowledgements We thank Dr. Dongxian Jiang (Department of Pathology, Zhongshan Hospital, Fudan University, Shanghai, China) and Dr. Weiyu Pan (Zhongshan Hospital, Fudan University, Shanghai, China) for their excellent pathological technology help.

Authors' contribution X. Huang, R. You, F. Liu, and Z. Jian contributed to acquisition of data, analysis and interpretation of data, statistical analysis, and drafting of the manuscript; G. Zhou, H. Yin, M. Wu, T. Sun, Z. Duan, W. Xu, S. Zhang, X. Yang, H. Jiao, S. Yang, and Q. Wang were involved in technical and material support; and L. Tan, J. Yin, H. Tang, and M. Lin contributed to study concept and design, analysis and interpretation of data, drafting of the manuscript, obtained funding, and study supervision. All authors read and approved the final manuscript.

Funding This study was funded by grants from National Natural Science Foundation of China (81902396), Zhongshan Hospital, Fudan University (2020ZSLC5, 2021ZSYQ27), Fujian Provincial Health Technology Project (2021GGB03), and Science and Technology Commission of Shanghai Municipality (23S31900400). All these study sponsors have no roles in the study design, in the collection, analysis, and interpretation of data.

Data availability Data and materials generated that are relevant to the results are included in this article. Other data are available from the corresponding author Prof. Tan upon reasonable request.

Declarations

Conflict of interest The authors declare that they have no competing interests.

Ethical approval This study was approved by the Clinical Research Ethics Committee of Zhongshan Hospital, Fudan University. Written informed consent was obtained from each patient.

References

1. Sung H, Ferlay J, Siegel RL, Laversanne M, Soerjomataram I, Jemal A et al (2021) Global cancer statistics 2020: GLOBOCAN estimates of incidence and mortality worldwide for 36 cancers in 185 countries. CA Cancer J Clin 71(3):209–249
2. Abnet CC, Arnold M, Wei WQ (2018) Epidemiology of esophageal squamous cell carcinoma. Gastroenterology 154(2):360–373
3. Watanabe M, Toh Y, Ishihara R, Kono K, Matsubara H, Murakami K et al (2022) Comprehensive registry of esophageal cancer in Japan, 2014. Esophagus 19(1):1–26
4. He Y, Liang D, Du L, Guo T, Liu Y, Sun X et al (2020) Clinical characteristics and survival of 5283 esophageal cancer patients: a multicenter study from eighteen hospitals across six regions in China. Cancer Commun (Lond) 40(10):531–544
5. Wong IYH, Lam KO, Zhang RQ, Chan WWL, Wong CLY, Chan FSY et al (2020) Neoadjuvant chemoradiotherapy using cisplatin and 5-fluorouracil (PF) versus carboplatin and paclitaxel (CROSS Regimen) for esophageal squamous cell carcinoma (ESCC): a propensity score-matched study. Ann Surg 272(5):779–785
6. Tang H, Wang H, Fang Y, Zhu JY, Yin J, Shen YX et al (2023) Neoadjuvant chemoradiotherapy versus neoadjuvant chemotherapy followed by minimally invasive esophagectomy for locally advanced esophageal squamous cell carcinoma: a prospective multicenter randomized clinical trial. Ann Oncol 34(2):163–172
7. Eyck BM, van Lanschot JJB, Hulshof M, van der Wilk BJ, Shapiro J, van Hagen P et al (2021) Ten-year outcome of neoadjuvant chemoradiotherapy plus surgery for esophageal cancer: the randomized controlled CROSS trial. J Clin Oncol 39(18):1995–2004
8. Liu J, Blake SJ, Yong MC, Harjunpaa H, Ngiow SF, Takeda K et al (2016) Improved efficacy of neoadjuvant compared to adjuvant immunotherapy to eradicate metastatic disease. Cancer Discov 6(12):1382–1399
9. Sun JM, Shen L, Shah MA, Enzinger P, Adenis A, Doi T et al (2021) Pembrolizumab plus chemotherapy versus chemotherapy alone for first-line treatment of advanced oesophageal cancer (KEYNOTE-590): a randomised, placebo-controlled, phase 3 study. Lancet 398(10302):759–771
10. Wang ZX, Cui C, Yao J, Zhang Y, Li M, Feng J et al (2022) Toripalimab plus chemotherapy in treatment-naive, advanced esophageal squamous cell carcinoma (JUPITER-06): a multicenter phase 3 trial. Cancer Cell 40(3):277-88e3
11. Luo H, Lu J, Bai Y, Mao T, Wang J, Fan Q et al (2021) Effect of camrelizumab vs placebo added to chemotherapy on survival and progression-free survival in patients with advanced or metastatic esophageal squamous cell carcinoma: the ESCORT-1st randomized clinical trial. JAMA 326(10):916–925
12 Yang Y, Tan L, Hu J, Li Y, Mao Y, Tian Z et al (2022) Safety and efficacy of neoadjuvant treatment with immune checkpoint inhibitors in esophageal cancer: real-world multicenter retrospective study in China. Dis Esophagus 35(11):doac031
13. Mohme M, Riethdorf S, Pantel K (2017) Circulating and disseminated tumour cells - mechanisms of immune surveillance and escape. Nat Rev Clin Oncol 14(3):155–167
14. Quail DF, Joyce JA (2013) Microenvironmental regulation of tumor progression and metastasis. Nat Med 19(11):1423–1437
15. Myers JA, Miller JS (2021) Exploring the NK cell platform for cancer immunotherapy. Nat Rev Clin Oncol 18(2):85–100
16. Green TL, Cruse JM, Lewis RE, Craft BS (2013) Circulating tumor cells (CTCs) from metastatic breast cancer patients linked to decreased immune function and response to treatment. Exp Mol Pathol 95(2):174–179
17. Kim CA, Bowie JU (2003) SAM domains: uniform structure, diversity of function. Trends Biochem Sci 28(12):625–628
18. Roberts AB, Russo A, Felici A, Flanders KC (2003) Smad3: a key player in pathogenetic mechanisms dependent on TGF-beta. Ann N Y Acad Sci 995:1–10
19. Li H, Fung KL, Jin DY, Chung SS, Ching YP, Ng IO et al (2007) Solution structures, dynamics, and lipid-binding of the sterile alpha-motif domain of the deleted in liver cancer 2. Proteins 67(4):1154–1166
20. Peters AE, Knopper K, Grafen A, Kastenmuller W (2022) A multifunctional mouse model to study the role of Samd3. Eur J Immunol 52(2):328–337
21. Li J, Chen Z, Tian L, Zhou C, He MY, Gao Y et al (2014) LncRNA profile study reveals a three-lncRNA signature associated with the survival of patients with oesophageal squamous cell carcinoma. Gut 63(11):1700–1710
22. Zhang X, Peng L, Luo Y, Zhang S, Pu Y, Chen Y et al (2021) Dissecting esophageal squamous-cell carcinoma ecosystem by single-cell transcriptomic analysis. Nat Commun 12(1):5291
23. Korsunsky I, Millard N, Fan J, Slowikowski K, Zhang F, Wei K et al (2019) Fast, sensitive and accurate integration of single-cell data with Harmony. Nat Methods 16(12):1289–1296
24. Chen B, Khodadoust MS, Liu CL, Newman AM, Alizadeh AA (2018) Profiling tumor infiltrating immune cells with CIBERSORT. Methods Mol Biol 1711:243–259
25. Huang L, Wu C, Xu D, Cui Y, Tang J (2021) Screening of important factors in the early sepsis stage based on the evaluation of ssGSEA algorithm and ceRNA regulatory network. Evol Bioinform Online 17:11769343211058464
26. Jin S, Guerrero-Juarez CF, Zhang L, Chang I, Ramos R, Kuan CH et al (2021) Inference and analysis of cell-cell communication using cell chat. Nat Commun 12(1):1088
27. Ritchie ME, Phipson B, Wu D, Hu Y, Law CW, Shi W et al (2015) limma powers differential expression analyses for RNA-sequencing and microarray studies. Nucleic Acids Res 43(7):e47
28. Yin J, Yuan J, Li Y, Fang Y, Wang R, Jiao H et al (2023) Neoadjuvant adebrelimab in locally advanced resectable esophageal squamous cell carcinoma: a phase 1b trial. Nat Med 29(8):2068–2078
29. Kato K, Cho BC, Takahashi M, Okada M, Lin CY, Chin K et al (2019) Nivolumab versus chemotherapy in patients with advanced oesophageal squamous cell carcinoma refractory or intolerant to previous chemotherapy (ATTRACTION-3): a multicentre, randomised, open-label, phase 3 trial. Lancet Oncol 20(11):1506–1517
30. van den Ende T, de Clercq NC, van Berge Henegouwen MI, Gisbertz SS, Geijsen ED, Verhoeven RHA et al (2021) Neoadjuvant chemoradiotherapy combined with atezolizumab for resectable esophageal adenocarcinoma: a single-arm phase II feasibility trial (PERFECT). Clin Cancer Res 27(12):3351–3359
31. Kelly RJ, Ajani JA, Kuzdzal J, Zander T, Van Cutsem E, Piessen G et al (2021) Adjuvant nivolumab in resected esophageal or gastroesophageal junction cancer. N Engl J Med 384(13):1191–1203
32. Shah MA, Bennouna J, Doi T, Shen L, Kato K, Adenis A et al (2021) KEYNOTE-975 study design: a phase III study of definitive chemoradiotherapy plus pembrolizumab in patients with esophageal carcinoma. Future Oncol 17(10):1143–1153
33. Habif G, Crinier A, Andre P, Vivier E, Narni-Mancinelli E (2019) Targeting natural killer cells in solid tumors. Cell Mol Immunol 16(5):415–422

34. Melaiu O, Lucarini V, Cifaldi L, Fruci D (2019) Influence of the tumor microenvironment on NK cell function in solid tumors. Front Immunol 10:3038
35 Tang F, Li J, Qi L, Liu D, Bo Y, Qin S et al (2023) A pan-cancer single-cell panorama of human natural killer cells. Cell 186(19):4235-51e20
36. Herault A, Mak J, de la Cruz-Chuh J, Dillon MA, Ellerman D, Go M et al (2024) NKG2D-bispecific enhances NK and CD8+ T cell antitumor immunity. Cancer Immunol Immunother 73(10):209
37. Wu C, Liu X, Liu R, Song S, Zheng ZF, Zeng Y et al (2025) Sustained endocytosis inhibition via locally-injected drug-eluting hydrogel improves ADCC-mediated antibody therapy in colorectal cancer. Adv Sci (Weinh) 12(2):e2407239
38. Skoulidis F, Araujo HA, Do MT, Qian Y, Sun X, Cobo AG et al (2024) CTLA4 blockade abrogates KEAP1/STK11-related resistance to PD-(L)1 inhibitors. Nature 635(8038):462–471
39. Vivier E, Rebuffet L, Narni-Mancinelli E, Cornen S, Igarashi RY, Fantin VR (2024) Natural killer cell therapies. Nature 626(8000):727–736
40. Luo J, Guo M, Huang M, Liu Y, Qian Y, Liu Q et al (2025) Neoleukin-2/15-armored CAR-NK cells sustain superior therapeutic efficacy in solid tumors via c-Myc/NRF1 activation. Signal Transduct Target Ther 10(1):78
41 Fontana P, Du G, Zhang Y, Zhang H, Vora SM, Hu JJ et al (2024) Small-molecule GSDMD agonism in tumors stimulates antitumor immunity without toxicity. Cell 187(22):6165-81e22